



Aeroacoustic analysis of various noise sources: comparison of jet nozzles on BeamformX

Carlos Imanol Hurtado Díez

Department of Mechanical, Materials and Aerospace Engineering

Under supervision of Dr. Ganesh Raman

Illinois Institute of Technology

Spring 2016 – Summer 2016



Index

Figure list.....	4
Summary.....	6
Introduction to noise and aeroacoustics	7
Tools and equipment for tests. BeamformX.....	10
Experiment setup	20
Results and analysis	22
Conclusions	38



Figure list

Figure 1: 3D all-direction sound propagation	6
Figure 2: Noise levels inside human hearing range	7
Figure 3: BeamformX opening screen.....	9
Figure 4: BeamformX single mic spectrum screen.....	10
Figure 5: BeamformX spectrogram	11
Figure 6: BeamformX display	12
Figure 7: BeamformX control screen	12
Figure 8: Display with/withput Optimav function.....	13
Figure 9: Control screen settings	14
Figure 10: Microphone and camera array.....	14
Figure 11: Compressed air jet and control valve.....	15
Figure 12: Manometer	15
Figure 13: Pressure-speed conversión	16
Figure 14: Insulation chamber	16
Figure 15: Jet nozzles 1	17
Figure 16: Jet nozzles 2	17
Figure 17: Nozzle naming.....	17
Figure 18: Teflon tape	18
Figure 19: Tuning fork	18
Figure 20: Experiment setup	19
Figure 21: 12 kHz spectrogram and spectrum	21
Figure 22: Tuning fork spectrum at impact moment and after 3 seconds	22
Figure 23: Tuning fork vibrations propagating.....	22
Figure 24: Tuning fork test spectrogram.....	23
Figure 25: Nozzles round vs Crown	24
Figure 26: Round vs crown 0.2M spectrum	24
Figure 27: Crown vs round display	25
Figure 28: Round vs crown, 0.3M spectrum	25
Figure 29: Crown vs round, 0.4M spectrum.....	26
Figure 30: Crown vs round, 0.5M spectrum.....	26
Figure 31: Blurriness comparison, narrow range (> 30 dB) vs wide range (> 1 dB)	27
Figure 32: Round vs crown 0.6M spectrum	27



Figure 33: Nozzle comparison: square big vs spear setup	28
Figure 34: Square big vs spear spectrum, 0.2M	28
Figure 35: Noise peaks source, 10kHz and 11.6kHz	29
Figure 36: Square big vs spear spectrum, 0.3M	29
Figure 37: Square big vs spear spectrum, 0.4M	30
Figure 38: 9.8 kHz peak source identification	30
Figure 39: Square big vs spear spectrum, 0.5M	31
Figure 40: Square big vs spear spectrogram, 0.5M	31
Figure 41: Square big vs spear spectrum, 0.6M	32
Figure 42: Squares comparison setup	32
Figure 43: Squares spectrum, 0.2M	33
Figure 44: Square comparison, noise source identification	33
Figure 45: Squares comparison spectrum, 0.3M	34
Figure 46: Squares comparison spectrum, 0.4M	34
Figure 47: Squares comparison, 0.4M spectrogram and source identification	35
Figure 48: Squares comparison spectrum, 0.5M	35
Figure 49: Squares comparison spectrum, 0.6M	36
Figure 50: Squares source identification, 0.6M	36



1. Summary

In this report, the reader will find a record and explanation of the work and experiments carried out as part of the 5 credits taken for “MMAE597: Special Topics” by the author during the Spring and Summer 2016 semesters at Illinois Institute of Technology, Chicago, under the supervision of Professor Dr. Ganesh Raman, of the Department of Mechanical, Materials and Aerospace Engineering, Armour College of Engineering.

This work revolves around the research in aeroacoustics: first an introduction to the concepts of noise, aeroacoustics and the importance of noise monitoring, identification and control will be presented.

After that, the main tool used in the experiments and measurements will be introduced: BeamformX, a cutting edge technology software that has been the principal asset and way to record, identify and quantify the various noise sources with which experiments have been conducted. The basics of this tool will be explained, with easy-to-understand explanations and graphics, so the reader can feel comfortable with the terminology and later results interpretation and plots.

Next, the necessary equipment, tooling and experiment setup will be explained, in order to get somehow standardized experiments and comparable results from one test to another, with the intention of showing how the experiments have been conducted and how they could be reproduced and further validated in future work. The reader will find two main sections of experiments: general tests, where simple noise sources will be analyzed, and have the intention of helping understand the basic concepts of aeroacoustics as well as the BeamformX software and getting used to the general equipment and methodology, and comparison of jet nozzles, where different shaped nozzles have been tested at different flow speeds with the use of a compressed jet facility.

With these, the experiment results will be presented in a comprehensible way, comparing the values obtained from one noise source to another and analyzing the reasons behind these results, extracting useful and reasonable cause-effect relationships and trends.

Last, some conclusions of the work done, both generally speaking and with regards to the specific experiments and results already commented, and some ideas for future works or research in the area are commented.



2. Introduction to noise and aeroacoustics

The vibration of an object or a surface, radiating pressure waves into the surrounding medium, usually generates sound. Sound waves are longitudinal mechanical waves traveling through air and having frequencies in the audible range. In addition to frequency, wavelength, and speed, another defining parameter for sound waves is intensity, defined as the average rate per unit area at which energy is transmitted by the wave:

Imaginary sphere area

$$A = 4\pi r^2$$

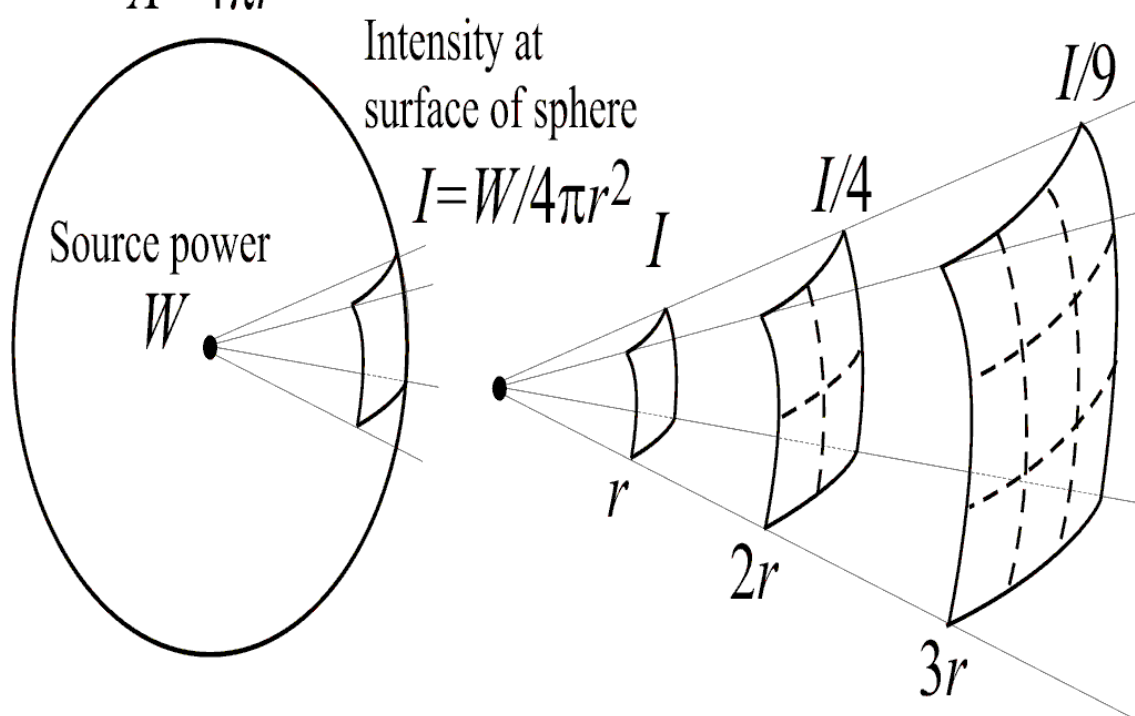


Figure 1: 3D all-direction sound propagation

But usually, instead of speaking of the intensity of a sound wave, it is more usual and convenient to talk about the sound pressure level (SPL), being the reason that the intensity of a sound varies with the square of its amplitude and it is impractical and uncomfortable to talk by means of intensity.

The sound pressure level is defined as:

$$SPL = 20 \cdot \log \frac{P}{P_{ref}}$$



Where SPL is measured in decibels (dB) and P_{ref} is 20 μ Pa, associated which is the lower limit of human hearing.

For humans, sound is the sensation produced at the ear by small pressure fluctuations in the surroundings (in most cases, air). On the other hand, noise can be defined as unwanted, uncomfortable, annoying or even painful sound. Quantifying and defining the threshold between bearable sound and noise is not easy, though, as it is a very subjective matter. However, a standardized approximate range of noises is commonly accepted, as follows:

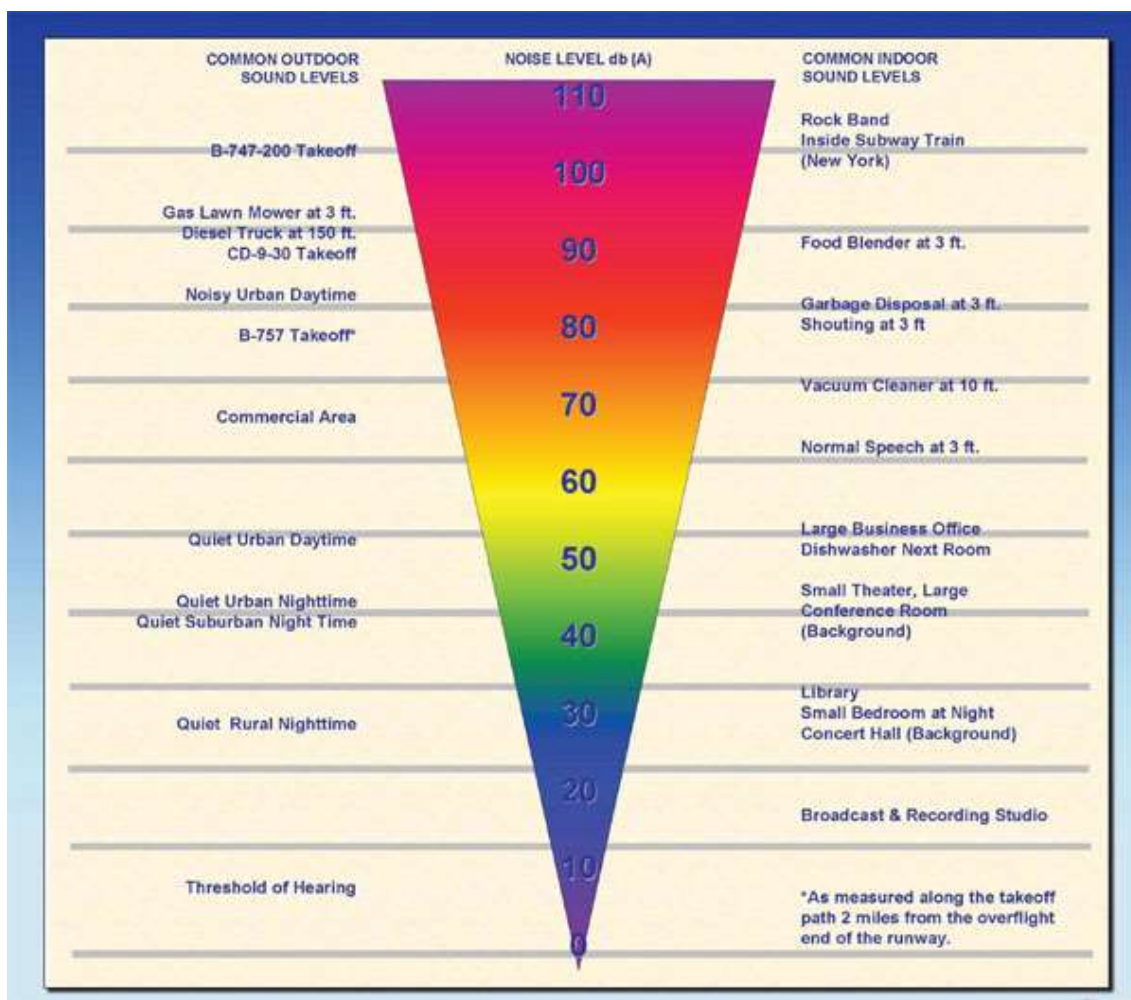


Figure 2: Noise levels inside human hearing range

Hence, noise control is a wide and important topic with application in many areas of both everyday life and the industry: from quieter engines for cars and other vehicles to improve the comfort of both passengers and pilots or the airplane industry, where it is ideal to have a quiet environment within the cabin to optimize the customer satisfaction in-flight (dampening is very important for this purpose) as well as for the inhabitants of airport surroundings.



In the industry, manufacturing quieter machines helps making the factory or workplace a more comfortable environment, boosting worker concentration and efficiency.

Besides, noise is often the sign of other phenomena: as explained, sound usually comes from a vibration, and vibratory effects are known to be dangerous in machinery, structures etc., possibly causing fatigue loadings and hence shortening their life cycle. Identifying the noise sources and making the necessary changes in design (geometry/shape, dampening location...) can be therefore a way to solve other problems of more tangible and destructive effects.

More recently, noise source identification and screening methods have been started to be experimentally applied and tested to be used in the fields of energy efficiency, insulation and leakage detection in buildings and others. Points where the sound can “leak” can also be areas where heat and energy can be lost.

Therefore, the importance of noise source identification, screening and analysis has been established.

On its side, the field of acoustics which studies the noise generation via a turbulent fluid motion and/or the interaction of this fluid with surfaces (and the subsequent aerodynamic forces) is called aeroacoustics. Aeroacoustics, for example, is the field where various noise sources can be studied best: jet outlets in airplanes, noise generated in the wind turbines... The first phenomena, for example, will be a case of study explained and recorded in this report, as will be seen later.

Last but not least, it is to be commented which parameters and measurements were taken in the following experiments: apart from the noise source spatial location itself, its intensity (in decibels, as explained), frequency ranges and spectrogram were taken, in order to make a full extensive study of the different noise sources, and not identify them just by their location.



3. Tools and equipment for tests. BeamformX

In this section, the different tooling and equipment used for the experiments will be introduced, with a special emphasis in the BeamformX software, vital for the attainment of these tests.

BeamformX is a software tool developed to be used in combination with an acoustic array system and a video camera. Noise tests and analyses can be done in a real-time way, or just recorded and saved for further post-processing and deeper analysis. Next, a short introduction to the software's interface will be presented so the reader can be comfortable with the different charts and graphics that will later be presented, as well as the different options that are provided for data processing and manipulation. The software version used and presented is 1.62, released on November 5, 2015.

First of all, the program must be opened. This is the first screen that the user receives:

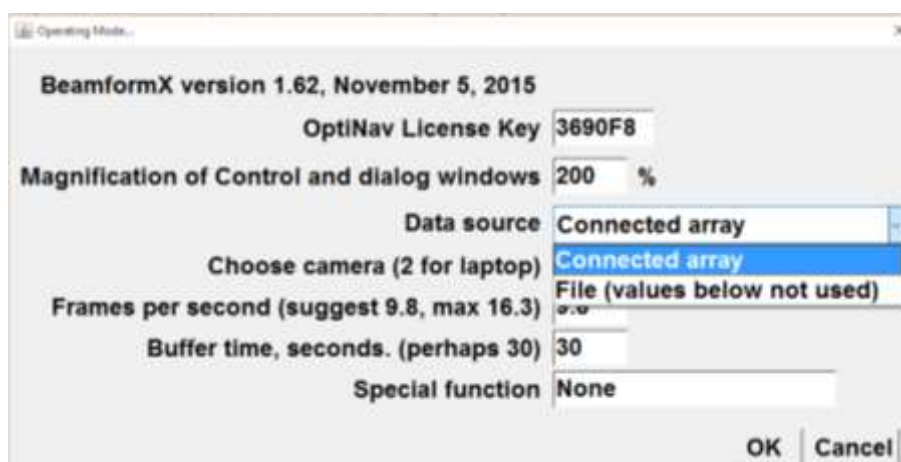


Figure 3: BeamformX opening screen

The most important option here is the “data source” selector: if the user is going to work on a real-time basis by using an existing microphone-camera array set, “Connected array” should be selected (of course, an array should be connected via USB with the computer). On the other hand, if the intention is to post-process some values already recorded and stored in the computer and work/analyze them, “File” should be selected. The frame/sec resolution and buffer time to be saved can be specified here, although as the program warns, those values below (such as frames per second etc.) are not used, as they are meant to be meaningful in the situation of using an array.

Once the application is opened and the work method chosen, 4 different screens are opened in the workspace:



- Screen 1: Single mic spectrum
 - The spectrum of a single mic is isolated, rather than the visual mapping that we can get from the complete array.
 - SPL Spectrum recorded by every microphone can be viewed.
 - Data can be plotted, recorded or saved as text file in this window.
 - It is different for every instant of the recording.

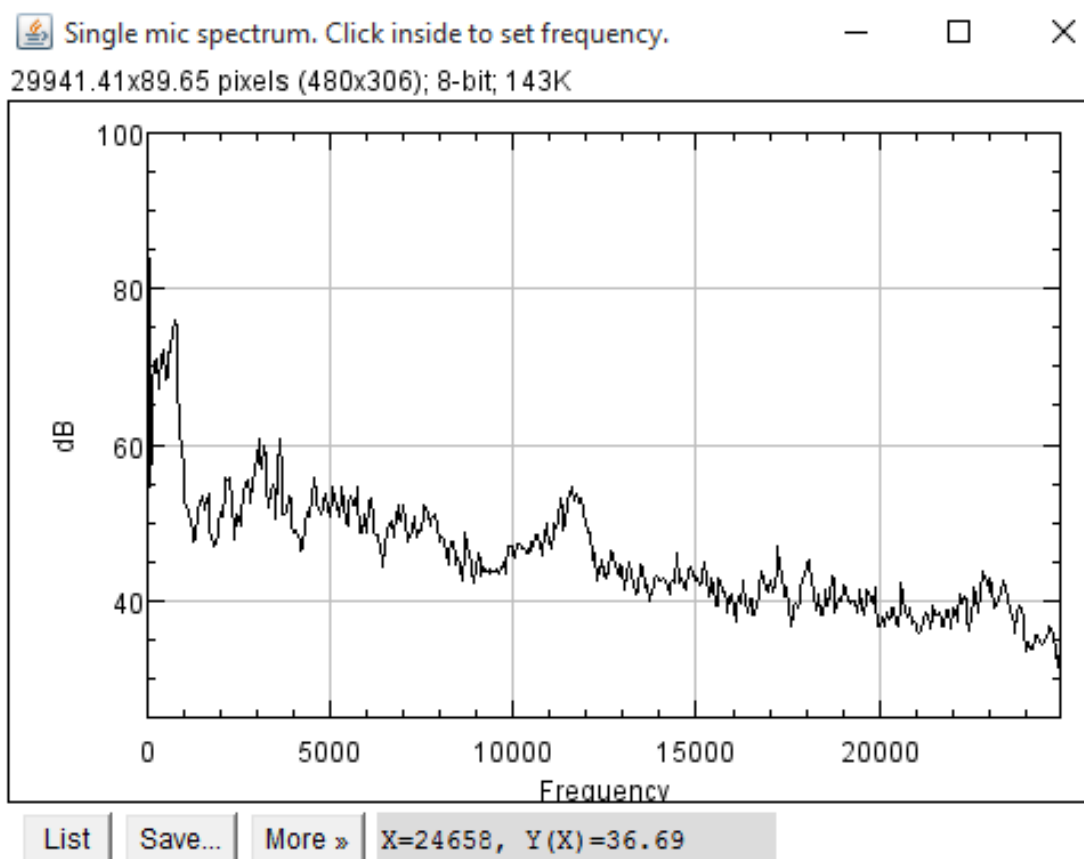


Figure 4: BeamformX single mic spectrum screen

- Screen 2: Spectrogram
 - It shows the amplitude and frequency information vs time. In order to make it easier for the user what to focus on at a particular point of time.
 - Bright points are noises of certain frequency that fall between the set range in the screen 4, control (explained later).
 - In the example, we can see that the loudest (in a set range of 45 to 90dB) noises come at relatively low frequencies between 0.5 and 3 kHz).

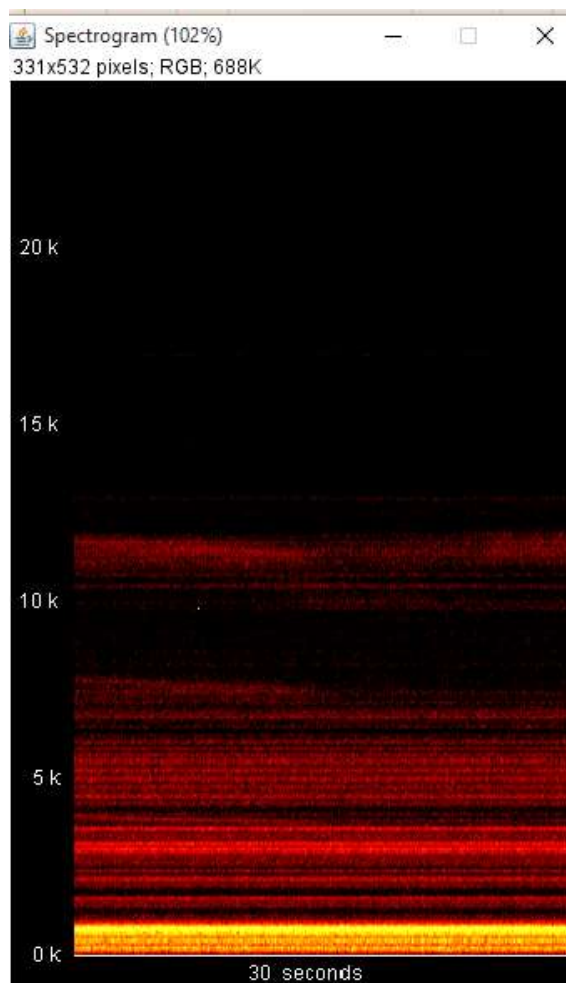


Figure 5: BeamformX spectrogram

- Screen 3: Display
 - This screen shows the real time beamforming images at the selected frequency and loudness range. It helps us locate the noise source effectively and understand whether we will be able to resolve the sources better or not.



Figure 6: BeamformX display

- Screen 4: Control
 - It is the main screen for BeamformX
 - It lets the user select frequency of interest, time of interest within the buffer time limit, loudness range, SPL levels to be shown inside the beamforming plot.

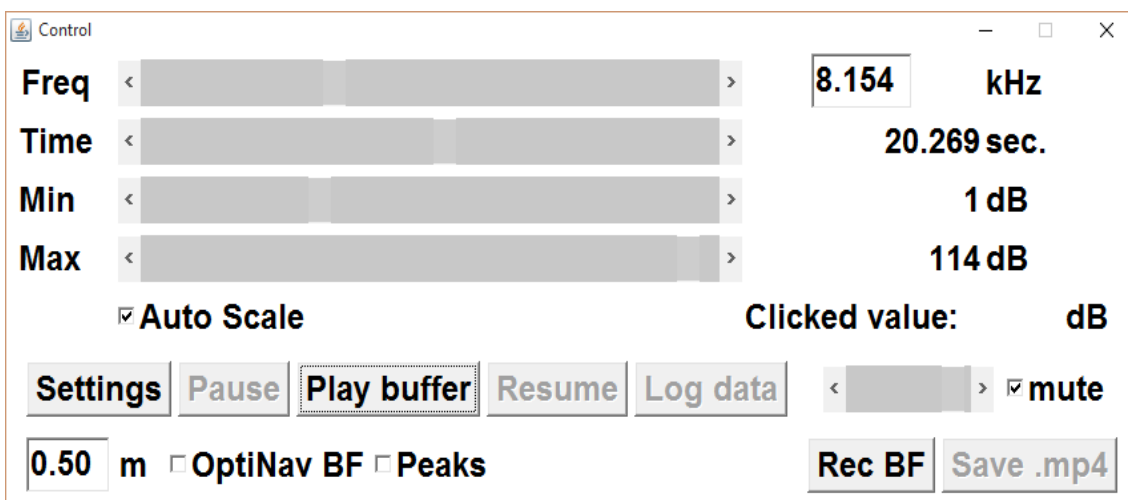


Figure 7: BeamformX control screen



- The control buttons:
 - Pause: Lets user pause the instantaneous beamforming.
 - Play buffer: Lets user playback the data in buffer time.
 - Resume: After pausing or viewing data in buffer time to continue.
 - Log data: Lets user record data (in the connected array work form).
 - Volume control & Mute: Control for the audio of the beamforming data.
 - Rec BF: To record the beamforming data file.
 - Save .avi: Lets user save video and audio files of the beamform data.
 - []m: Distance between array and source (necessary for the program to make the interpolation that makes the visual mapping possible).
- Optimav BF: optimizes the location and tries to isolate secondary vibrations and environmental reverb from the actual noise sources.

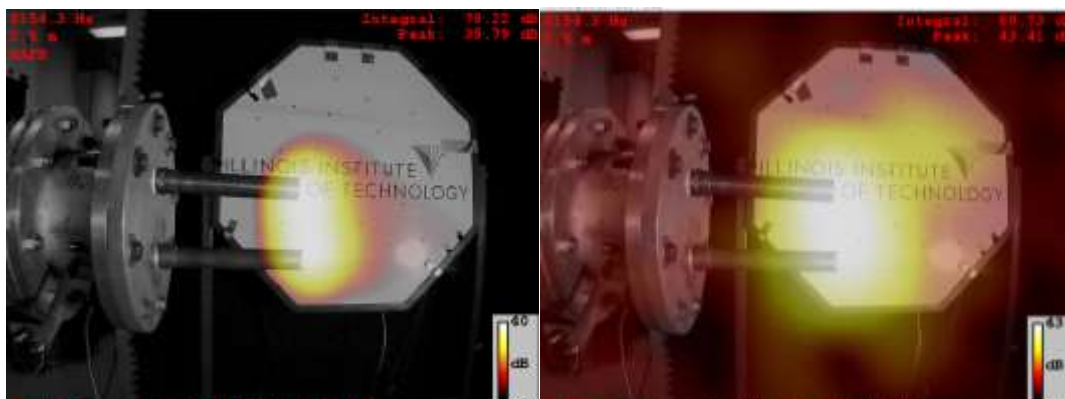


Figure 8: Display with/withput Optimav function

- Peaks function: to show only the noise peaks at stablished frequency.



Settings on Control screen: In the following image can be seen some of the options and settings that can be accessed from the Control screen, but need no further explanation.

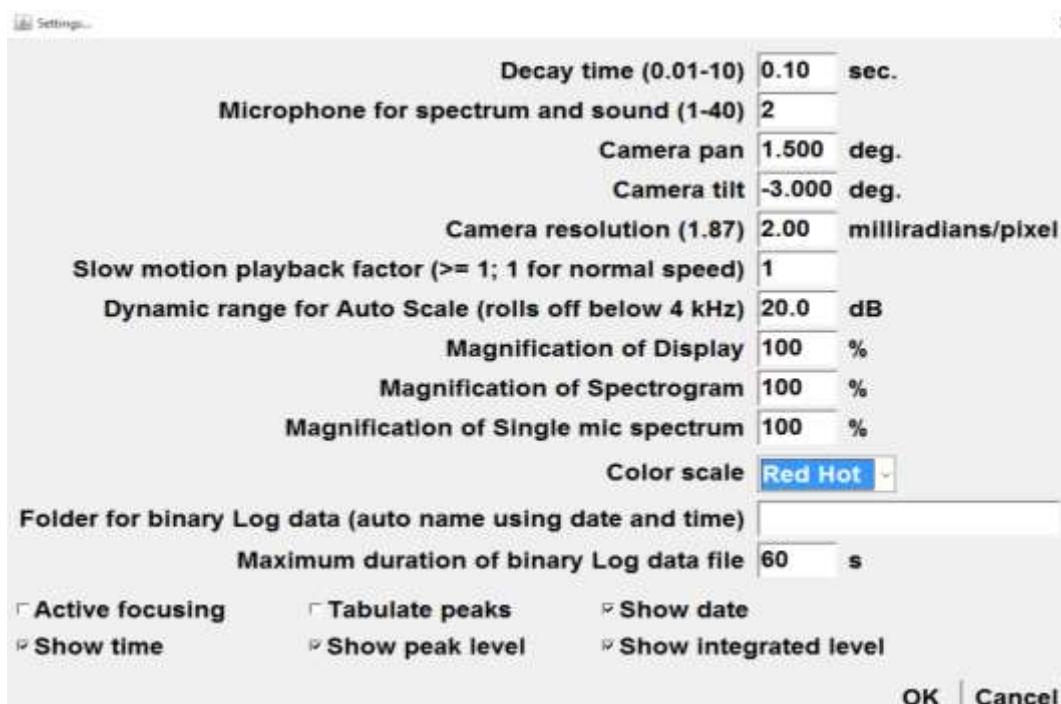


Figure 9: Control screen settings

Now the rest of the equipment and apparels for the experiments will be commented, apart from the BeamformX software tool, present in all of the experiments:

1. Microphone and camera array: This is a 2-dimensional microphone array of 64 microphones and a camera, set up on an 8-by-8 grid, with the camera in the center. Thanks to the various microphones, and given the distance from the array to the expected noise source, the program algorithm will be able to conform a visual mapping of the situation, as has been seen.



Figure 10: Microphone and camera array



2. Compressed jet air facility: This facility will provide the air flow necessary for the aeroacoustic tests and to simulate the jet engine outlets. The air flow can be regulated with a valve, and flow speeds from 0 to 1.3 Mach can be achieved (after 0.8M compressibility effects start appearing). The facility has 2 threaded holes at the end of it to where different nozzles can be placed.



Figure 11: Compressed air jet and control valve

3. Electronic manometer: connected to the compressed air jet facility, measures the pressure of the flow in pounds per square inch (psi) and hence the speed of the flow is determined. For this, standard conditions are supposed in the lab ($T = 298K$).



Figure 12: Manometer



Flow pressure (psi)	Flow speed (Mach number)	Flow speed (cm/s)
20.95	1.2	365.8
16.69	1.1	341.54
13.13	1.0	315.88
10.16	0.9	288.9
7.71	0.8	260.64
5.69	0.7	231.16
4.05	0.6	200.52
2.74	0.5	168.85
1.71	0.4	136.25
0.95	0.3	102.88
0.42	0.2	68.93

Figure 13: Pressure-speed conversión

4. Insulation chamber: This is the physical space in where the experiments were conducted. It is a specifically designed chamber with damping and insulation in the walls, in order to minimize the possible reverb effects with the environment and secondary noise sources that may occur, so the results are cleaner and not distorted.



Figure 14: Insulation chamber

5. Jet nozzles: These are the different nozzles that are used to compare and asses the aeroacoustic noise that different geometry outlets cause at different airflow speeds. They consist of cylindrical copper-body tubes with different geometry heads. As commented earlier, they can be attached in the threaded holes of the compressed jet air outlets two by two.



Figure 15: Jet nozzles 1



Figure 16: Jet nozzles 2

From left to right, these is the denomination that will be used from now on when naming the nozzles:

- | |
|---------------|
| Square up |
| Square big |
| Square medium |
| Square small |
| Spear |
| Round |
| Crown |

Figure 17: Nozzle naming



6. Teflon tape: When the different nozzles are attached to the compressed air jet facility, their threads must be covered with Teflon tape in order to prevent air leaks and hence disturbances on the flow and measure.



Figure 18: Teflon tape

7. Tuning fork: A tuning fork is an acoustic resonator used in musical applications to tune instruments and other tools. Its special geometry makes it vibrate at 440Hz when receiving an impact type of action. The object is then located in such way that the ball in one of the extremes touches instruments and transmit these vibrations, making it sound. In this context, tuning forks are designed to vibrate at 440 Hz as this frequency corresponds with the note A (3rd string in a violin).

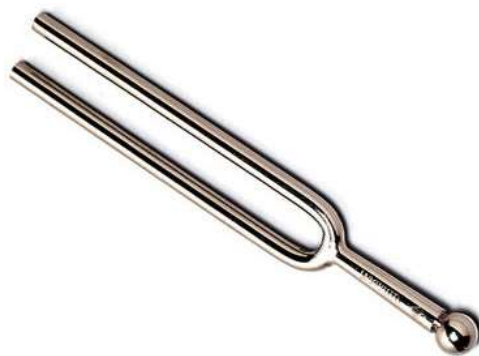


Figure 19: Tuning fork



4. Experiment setup

All experiments were set up and carried out in a similar fashion:

1. Noise source is placed in the insulation chamber at an appropriate height to enter the camera span.
2. Sufficient lighting is given for the camera to get clear images, with a lamp or other source.
3. Camera and array set are located in the insulation chamber, and the distance from it to the noise source measured, and entered in the BeamformX.
4. The noise source is run and measurements taken, both in video and in .log format, for later analysis.



Figure 20: Experiment setup

There were a total of 18 experiments carried out:

- a) Noise source of 12 kHz. Distance 1 m.
- b) Tune fork at 440 Hz. Distance 2 m.
- c) Nozzle comparison: round vs crown. Distance 1 m.
 - a. 0.2M
 - b. 0.3M
 - c. 0.4M
 - d. 0.5M



- e. 0.6M
- d) Nozzle comparison: square big vs spear. Distance 1 m.
 - a. 0.2M
 - b. 0.3M
 - c. 0.4M
 - d. 0.5M
 - e. 0.6M
- e) Nozzle comparison: square small vs square big. Distance 1 m.
 - a. 0.2M
 - b. 0.3M
 - c. 0.4M
 - d. 0.5M
 - e. 0.6M

The first case of analysis, with the stationary 12 kHz source, had the intention of testing and starting to get familiar with the BeamformX software and the testing procedures. A smartphone was used to get the source, playing a 12 kHz recorded frequency.

The tuning fork was judged interesting to analyze, in order to see what other vibration frequencies were produced with an impact load on the object, and how these vibrations were transmitted to other objects (a wooden panel) as well as the decay time.

In the case of nozzle comparisons, the intention was to assess the aeroacoustic noises created by the interaction of a fast air flow with the surfaces and the comparison of these noise with respect to the geometry of the nozzle itself, the frequency, and intensity (dB), as well as how these change with the change in flow speed, always between 0.2M to 0.6M (as explained before, it was decided not to go beyond that 0.6M threshold for security reasons, as the valve in the compressed air facility is not in the best condition and a higher speed flow could be a risk).



5. Results and analysis

- 1) Noise source of 12 kHz: This was the first experiment carried out, which main intention was to start understanding and “playing” with the BeamformX software controls. Being so, a source creating a noise of 12 kHz (a smartphone playing a recording of that frequency) was located inside the insulation chamber, and measured. It was to be measured whether the source was indeed producing noise at 12 kHz, and at what intensity, and if there were non-negligible frequencies of other kind. Here the spectrogram and single mic spectrum:

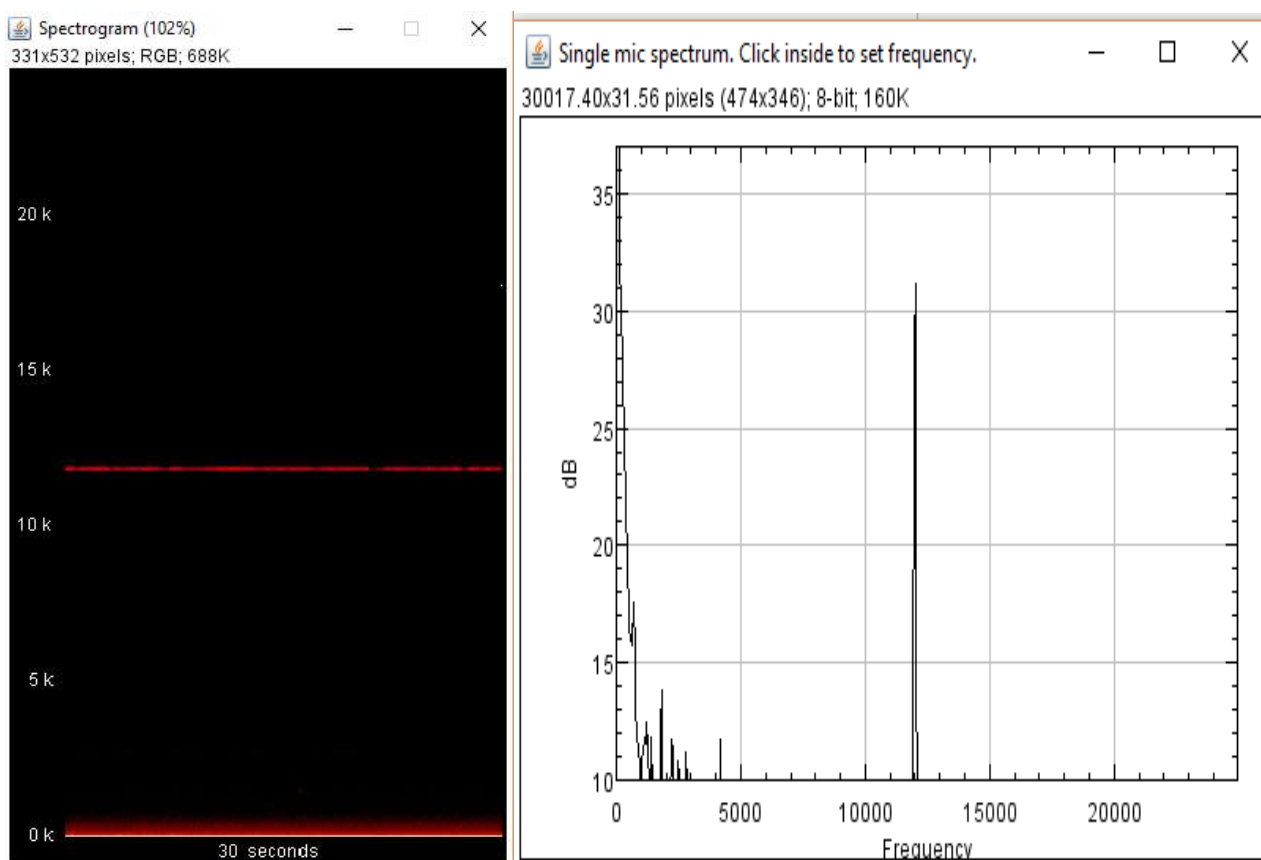


Figure 21: 12 kHz spectrogram and spectrum

As expected, there is a sustained 12 kHz measurement throughout all the recording, at an intensity of 32 dB (intensity was limited in the control panel to the 1 dB – 100 dB range, and the spectrum zoomed in order to get a better view of the intensities). Still, there is some noise coming at low frequencies and relatively low intensities. Obviously, the 12 kHz had its origin in the smartphone placed, but after a study in the display to locate the low frequencies sources, it appeared clear that this was background environmental noise coming from contiguous rooms, piping and HVAC system, and the computer’s fan itself.



2) Tuning fork: In this second experiment, a tuning fork was subject to an impact load and hence vibrated at a 440 Hz frequency. However, at the exact moment of the impact, many more frequencies are provoked, at audible ranges. Soon afterwards, anyway, these noises and vibrations fade away (after about 1.5 seconds) and only the expected 440 Hz vibration remains:

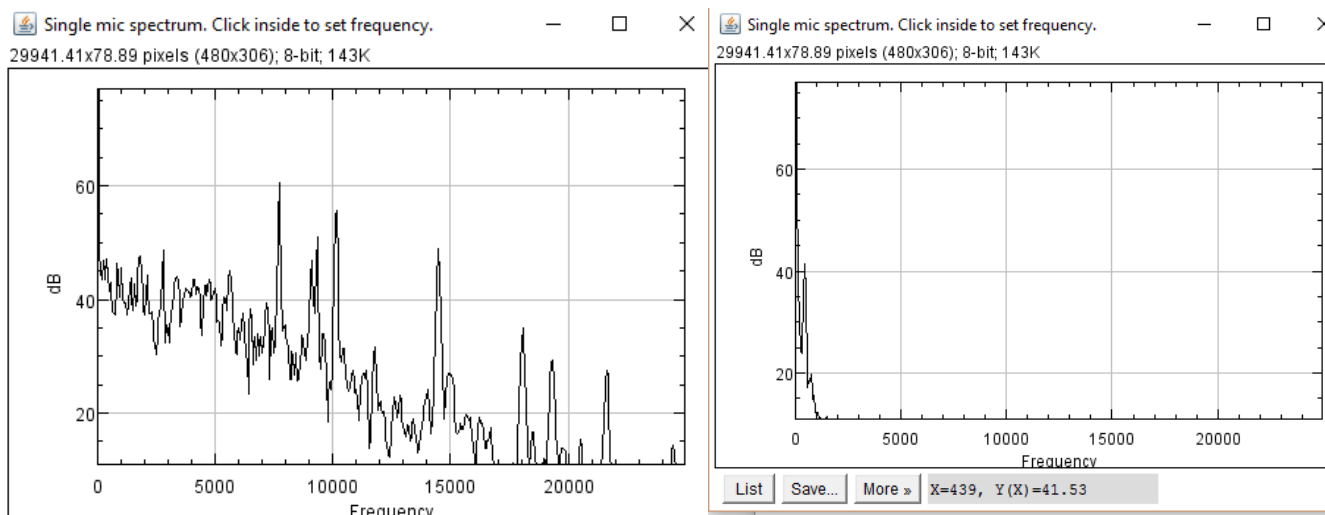


Figure 22: Tuning fork spectrum at impact moment and after 3 seconds

As explained, after vibrating the tuning fork is put in contact with a board to which it transmits the vibrations. It was tested putting it at the different corners of the board, where vibrations spread and died out from the contact point. For example, when located at one of the corners, vibrations propagate in a circular-way fashion:

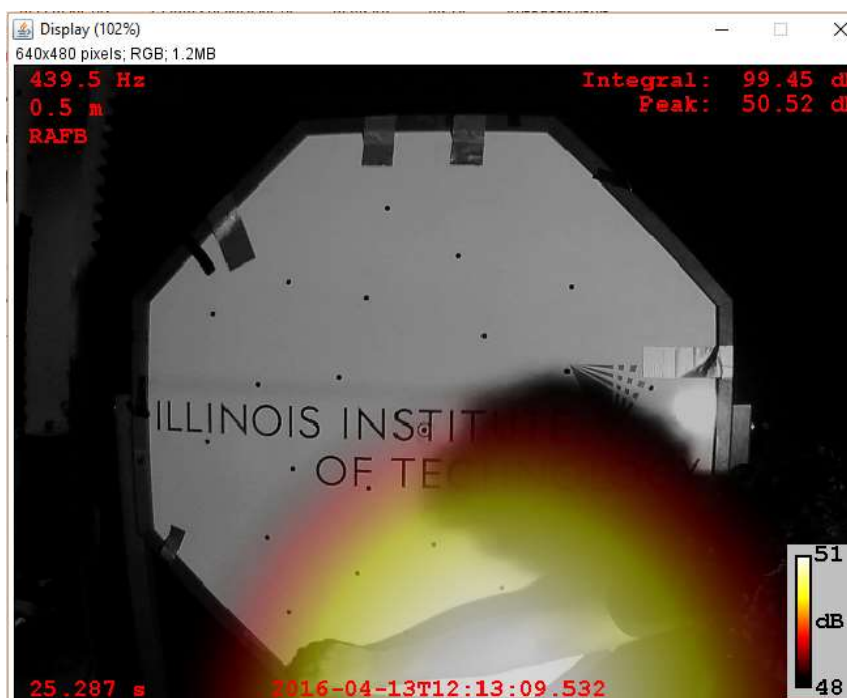


Figure 23: Tuning fork vibrations propagating



But maybe the most interesting data that can be extracted is that coming from the spectrogram. With it, the time necessary for the noise to die out can be deduced (in the controls, range of 1 to 80 dB specified):

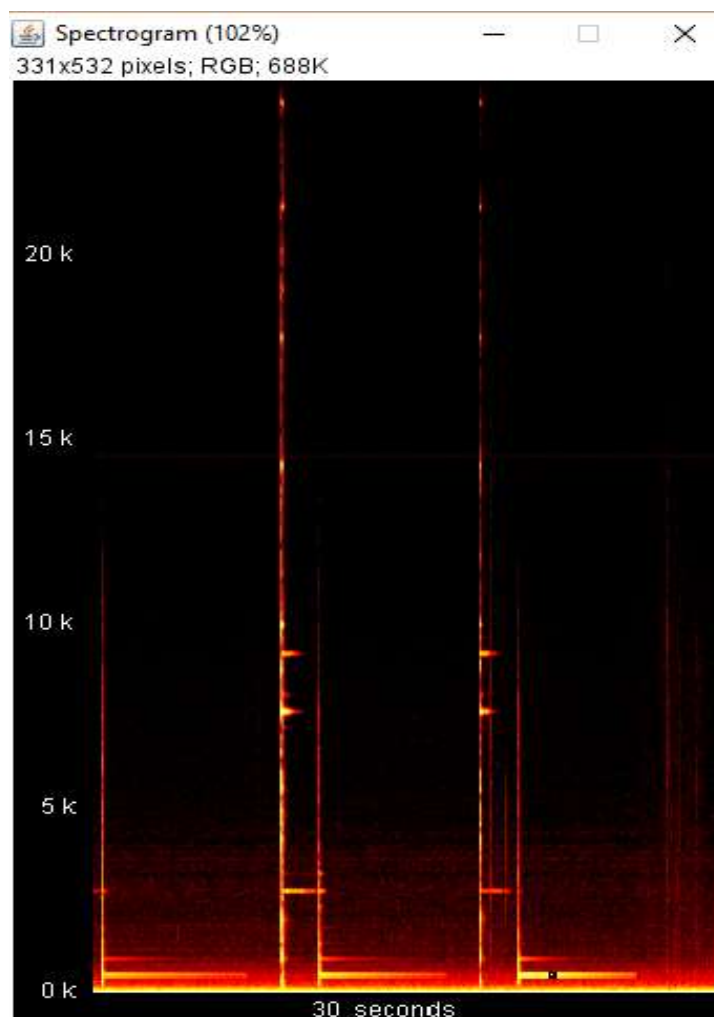


Figure 24: Tuning fork test spectrogram

There is a clear repetitive pattern that can be appreciated and explained as follows: the first, “tall” bright column corresponds to the moment of the impact load on the tuning fork, where (as explained) many different frequency ranges are excited all at once but immediately fade away. The next bright column is when the tuning fork is put in contact with the board, and as we see the 440 Hz frequency vibration is here the most important one and for the longest time (although a vibration near the 900 Hz is also excited and sounds for a shorter time). In all cases, and placed in all tested points of the board, the noise takes approximately **8 seconds** to fade away (get mixed and non-differentiable with background noise), from an initial 40 dB (approximately).



With this, we will start presenting the core part of the experiments carried out, this is, the different geometry nozzle comparison. Sometimes some data will be omitted if found superfluous or not adding any valuable or new information to whatever has been commented in previous cases. Being the flows steady, conditions and results are also considered steady (experiments prove this as a reasonable assumption) so the time factor will not be taken into account. For each cases, flow speeds ranging from 0.2 to 0.6M have been tested.

3) Nozzle comparison: round vs crown.

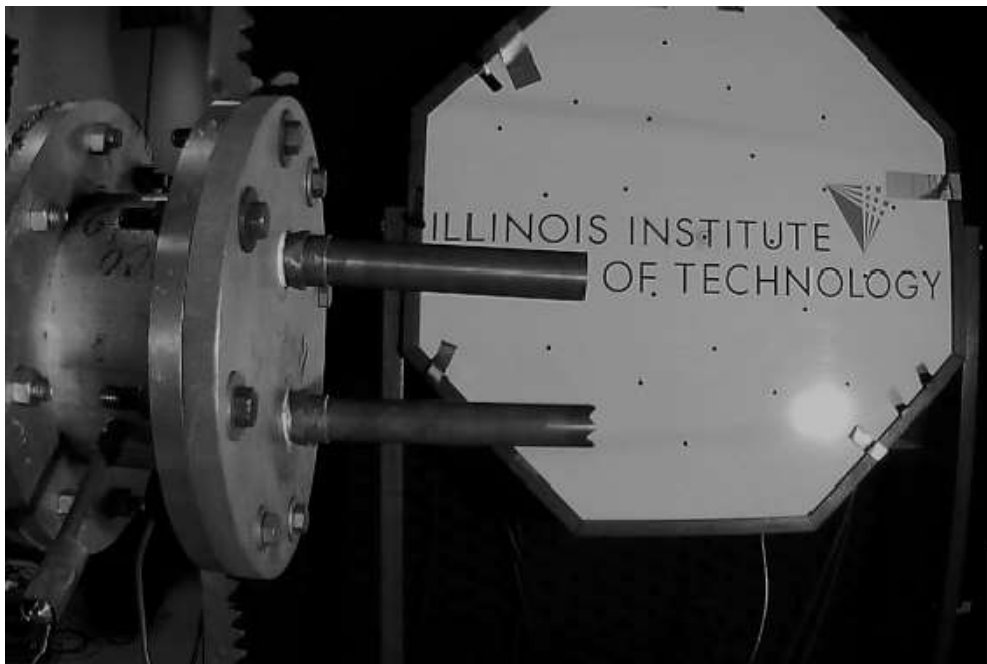


Figure 25: Nozzles round vs Crown

3.1) 0.2M:

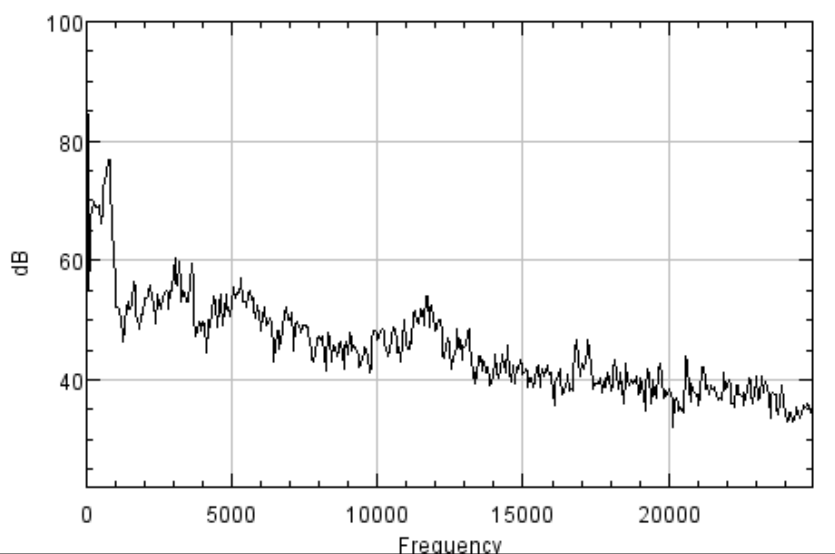


Figure 26: Round vs crown 0.2M spectrum



The loudest noise (78 dB) happens at around 800 Hz, but it is interesting to comment that, even though many peaks are present, there is a downwards trend, so the experiment begins with noises ranging 50 – 78 dB at low frequencies (< 1 kHz) but at high frequencies (>25 kHz) it barely goes over 30 dB . By studying the graphic display, there is another interesting effect that can be seen: at low and medium frequencies, the crown geometry nozzle appears to be a source of louder noise, but there is no appreciable difference when analyzing the higher frequencies:

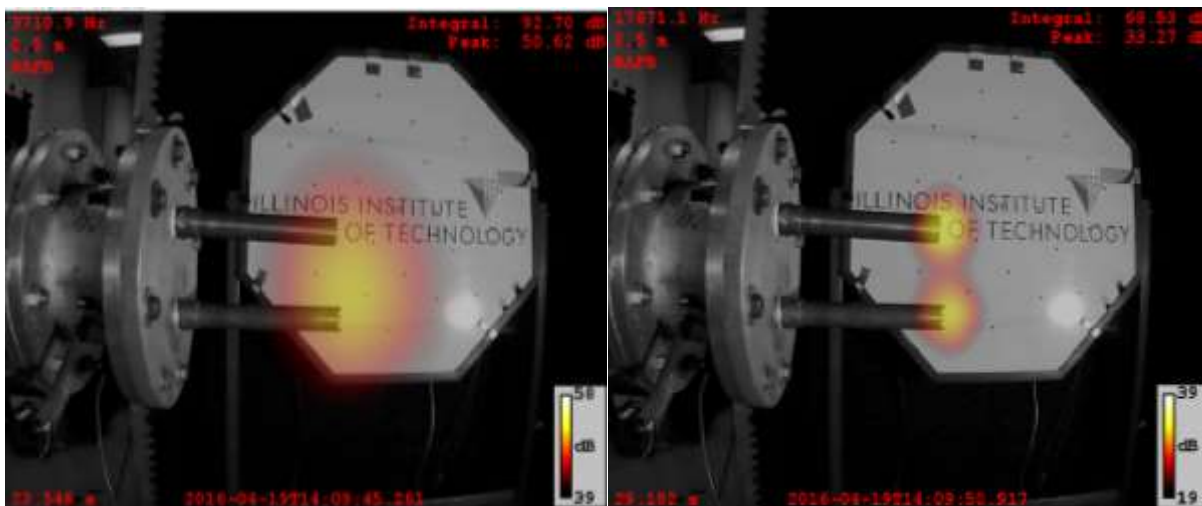


Figure 27: Crown vs round display

3.2) 0.3M:

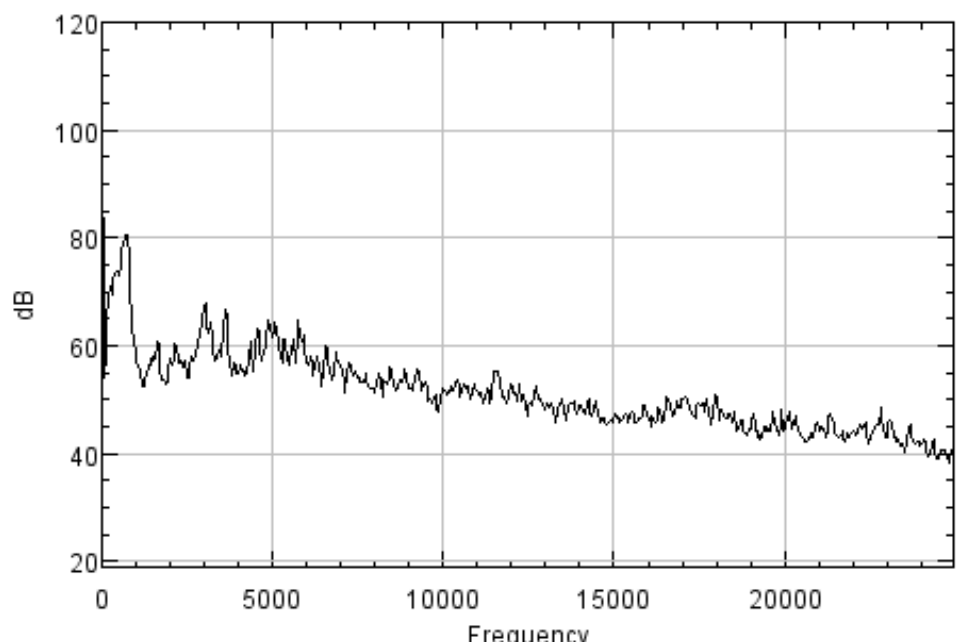


Figure 28: Round vs crown, 0.3M spectrum

It can be observed how the trend in peaks and loudness distribution is exactly the same, but as the flow speed has increased, so has the noise range (now the lowest noises never go below



40dB, and more than 80 dB are reached at other parts). With regards to the display, the same type of behavior can be appreciated, being the crown-headed nozzle louder in general.

3.3) 0.4M:

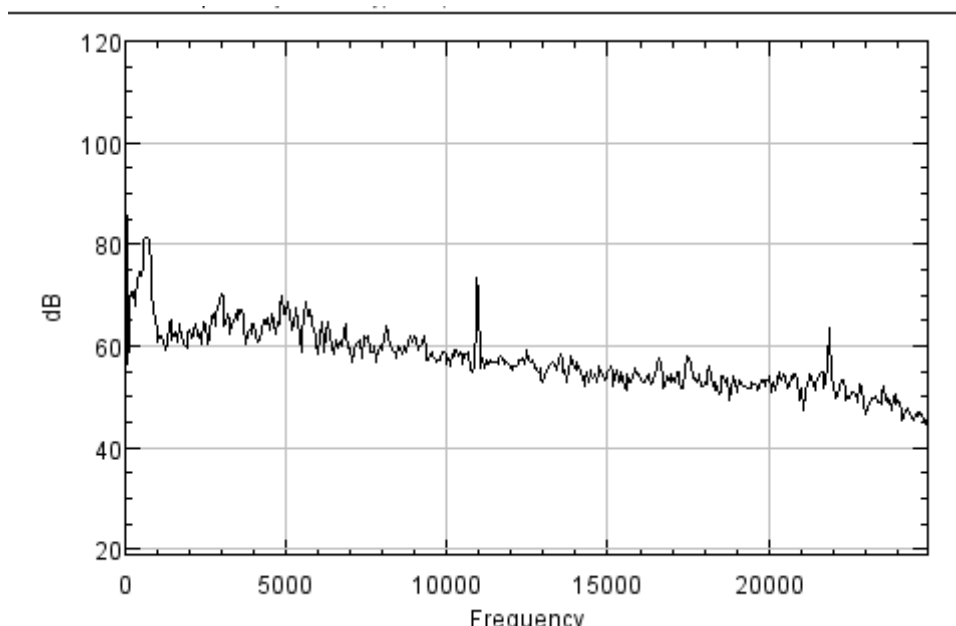


Figure 29: Crown vs round, 0.4M spectrum

Although the trend is similar as speed goes higher, it is interesting to point out how a less spiky line is formed in the spectrum, and although there is still a downward tendency, this line is more horizontal than when speed was 0.2M, meaning that the loudness increase is sharper the higher the frequency, while it remains quite steady at low frequencies. This trend will be confirmed shortly.

3.4) 0.5M:

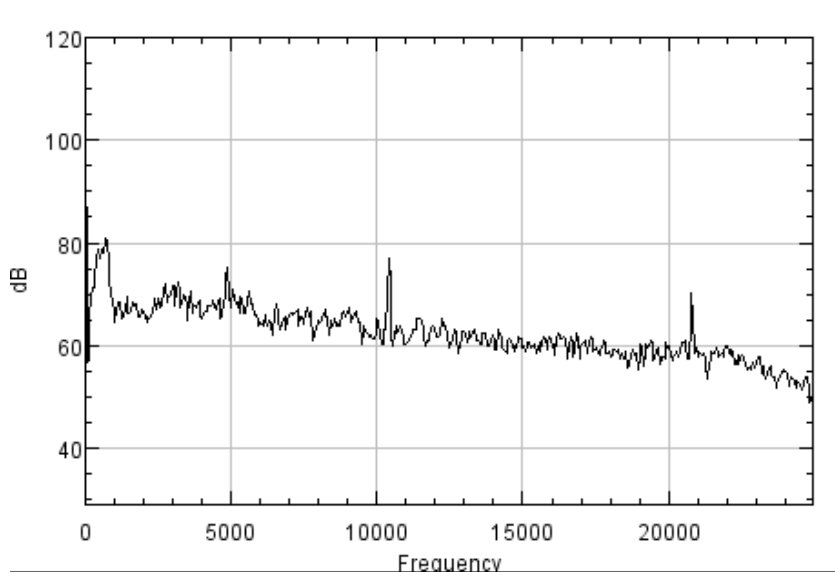


Figure 30: Crown vs round, 0.5M spectrum



Indeed, the observed effect and observations already commented seem to be correct, for the minimum noise has risen another 5 dB from the previous flow speed, but the maximum is still near the 80 dB. With regards to the display, there is nothing new or noteworthy to comment, just the predictable way the noise expands in a longer distance in the flow. Furthermore, as some of the noises get louder with flow speed, the range must be set narrower in the control panel in order to see more clearly the sources, otherwise the image gets blurrier and useless. For example:

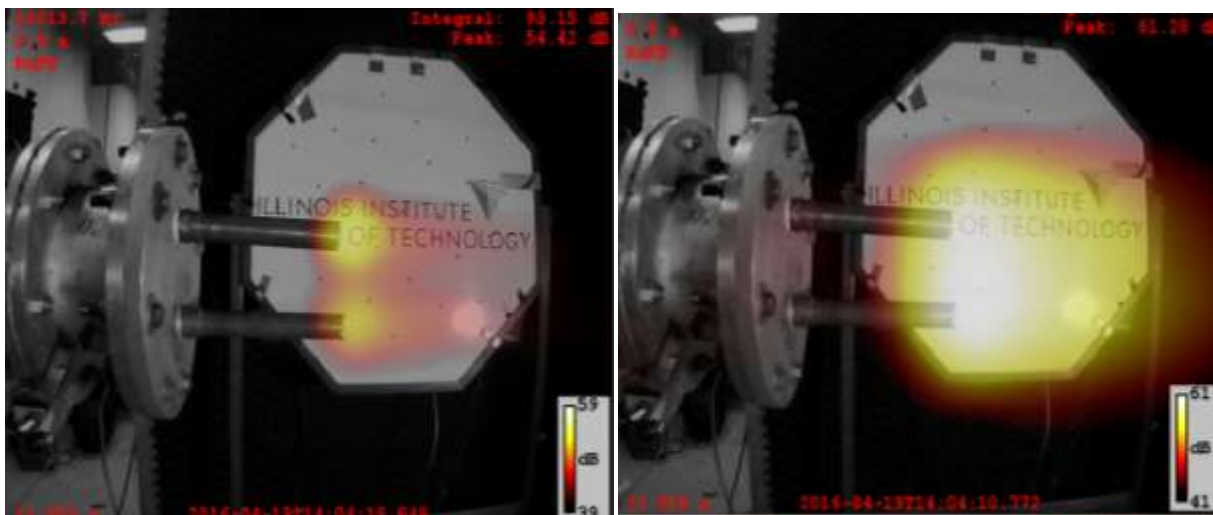


Figure 31: Blurriness comparison, narrow range (> 30 dB) vs wide range (> 1 dB)

3.5) 0.6M:

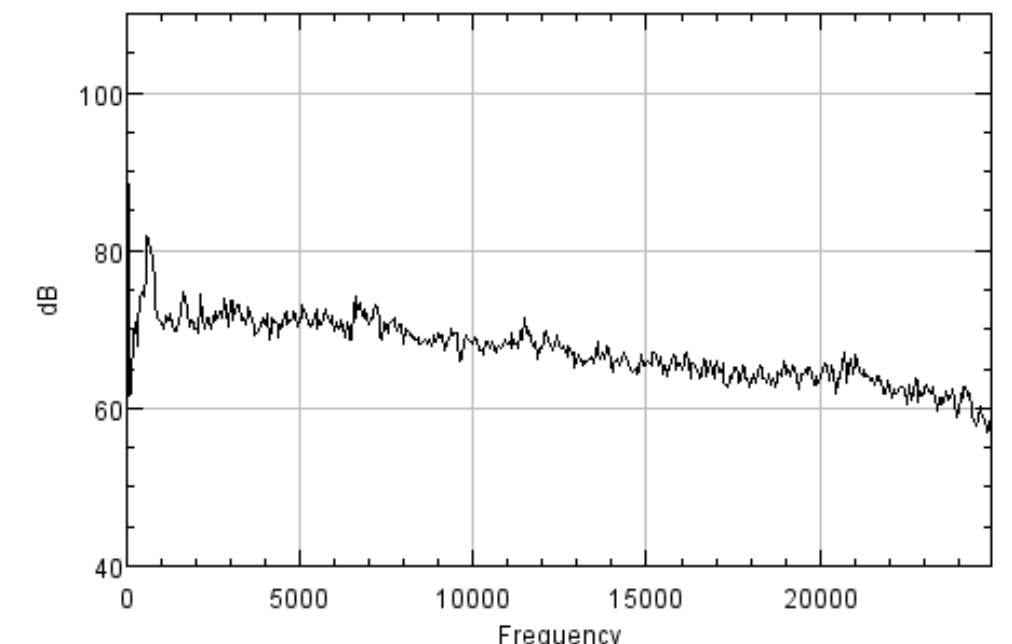


Figure 32: Round vs crown 0.6M spectrum



After presenting the results and different spectrums, plots and displays, it appears clear how with these nozzles there is some low frequency noise that remains almost independent of the flow speed (and at approximately 80 dB) while the noise level is more dependent of the flow speed, the higher the flow speed (starting from ≈ 25 dB at 0.2M to ≈ 60 dB at 0.6M), which can lead us to think that this trend will continue as speed increases and might equal or even surpass the 80 dB boundary of the lower frequencies at some speed close to the 0.75M, although compressibility effects may start arising and more experiments should be carried out in that space. With regards to the noisiest nozzle, the crown-headed nozzle is louder generally speaking in all conditions, having more outlet contact perimeter with the flow.

4) Nozzle comparison: square big vs spear.

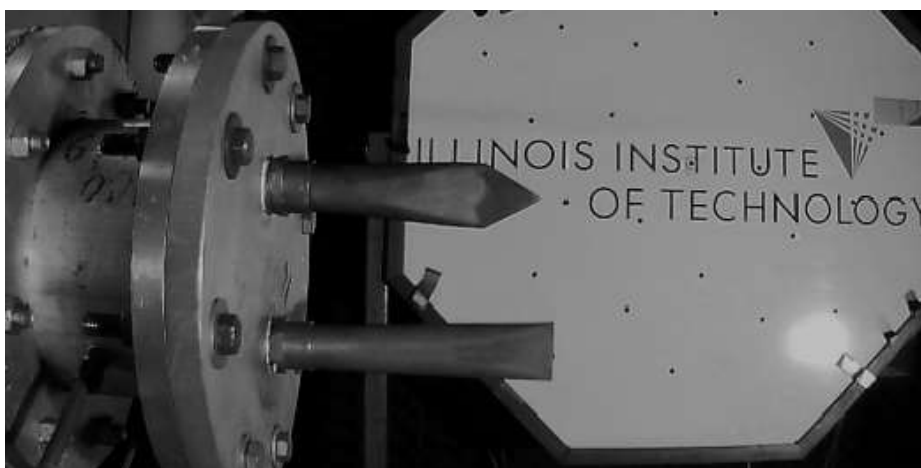


Figure 33: Nozzle comparison: square big vs spear setup

4.1) 0.2M:

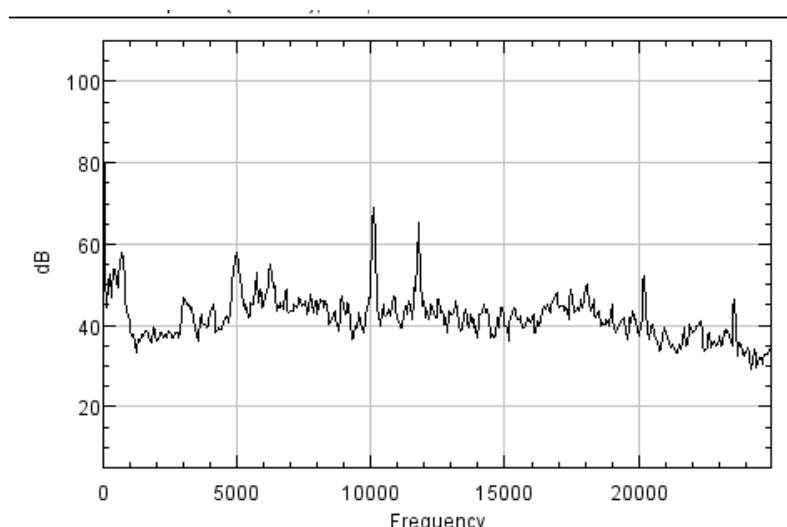


Figure 34: Square big vs spear spectrum, 0.2M



In this case, we can see that the noises created have a more “horizontal” tendency, although still very high frequencies are not as loud as very low ones (35 dB versus almost 60 dB). However, in the normal spiky shape of the spectrum, two interesting and higher spikes can be appreciated, that reach the 70 dB intensity, at about 10 and 12 kHz). If analyzed in the display, we can appreciate how these noise spikes are coming from the spear geometry nozzle:

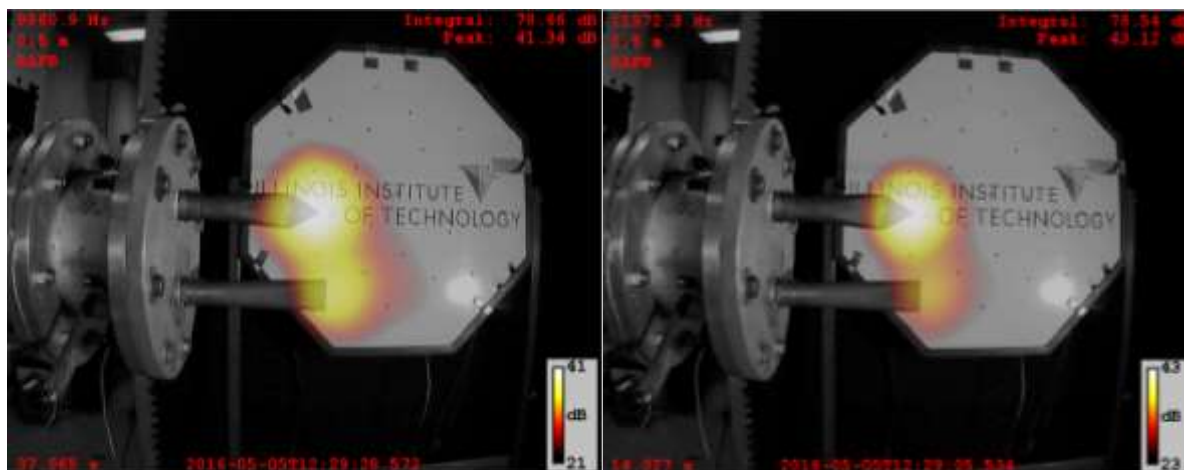


Figure 35: Noise peaks source, 10kHz and 11.6kHz

Overall, the spear geometry nozzle is noisier than the square, not only by creating the peaks but also generally speaking throughout all the frequency spectrum, although at low frequencies the display becomes blurry and difficult to identify.

4.2) 0.3M:

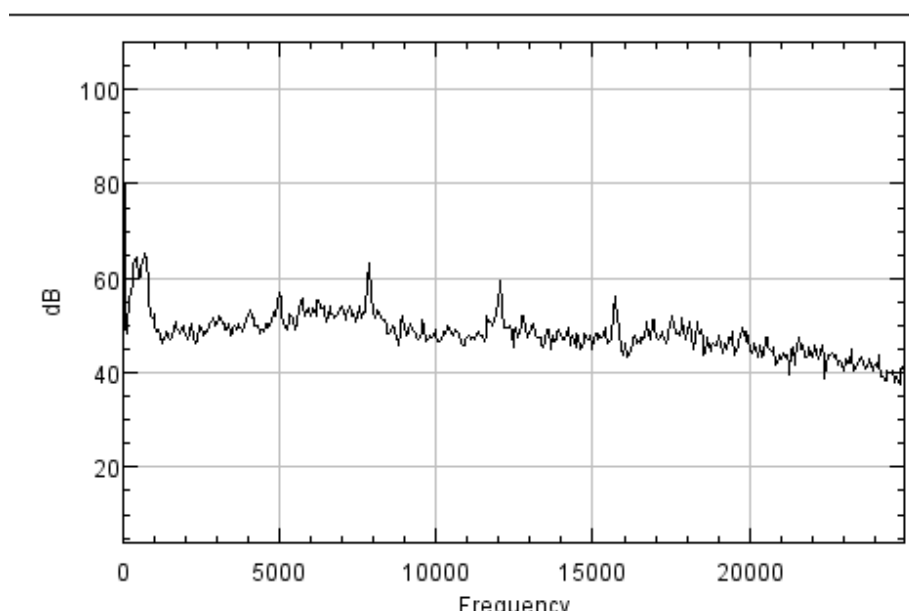


Figure 36: Square big vs spear spectrum, 0.3M



Surprisingly, the peaks that could be found at 0.2M have disappeared from the spectrum and the pattern is more horizontal. However, there is a noticeable increase in the general “average” noise intensity, from 40 dB to 45-50 dB approximately.

4.3) 0.4M:

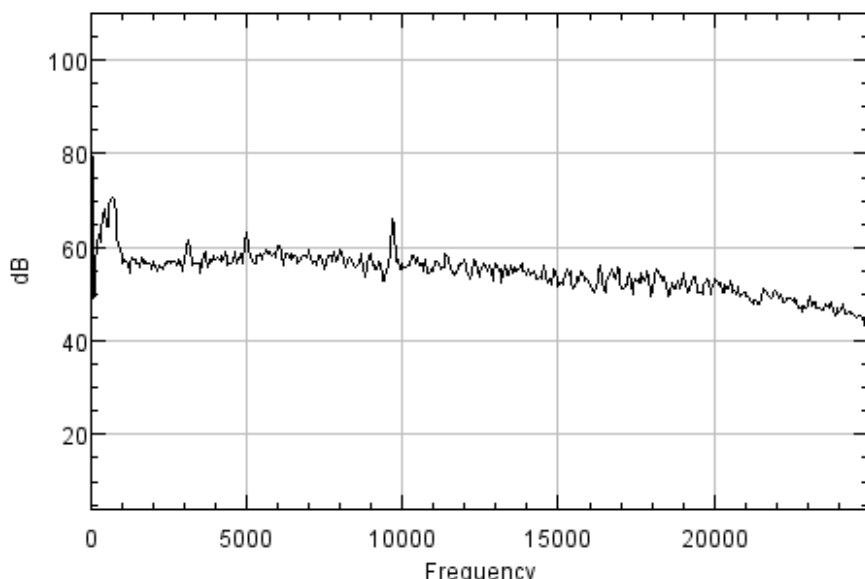


Figure 37: Square big vs spear spectrum, 0.4M

There is not noteworthy change in the tendency and shape of the spectrum, although all values increase about 5 dB from the 0.3M speed case.

If so, the most interesting point is the small peak around 9.8 kHz that is sustained over time. If observed more closely, we can see how this comes from the spear (narrowing the range to appreciate it better):

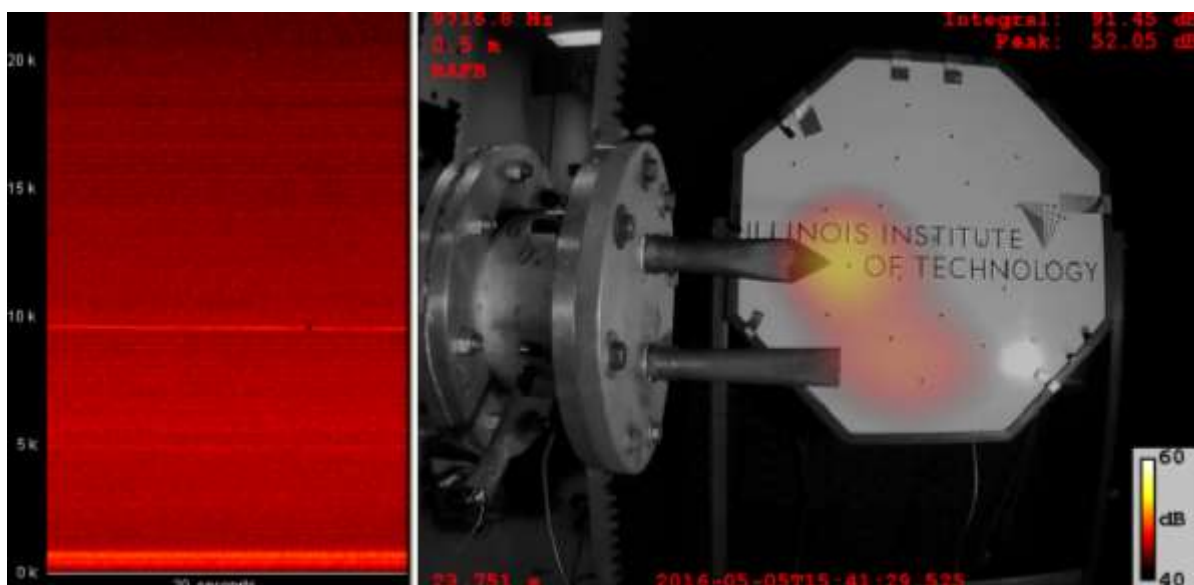


Figure 38: 9.8 kHz peak source identification



4.4) 0.5M:

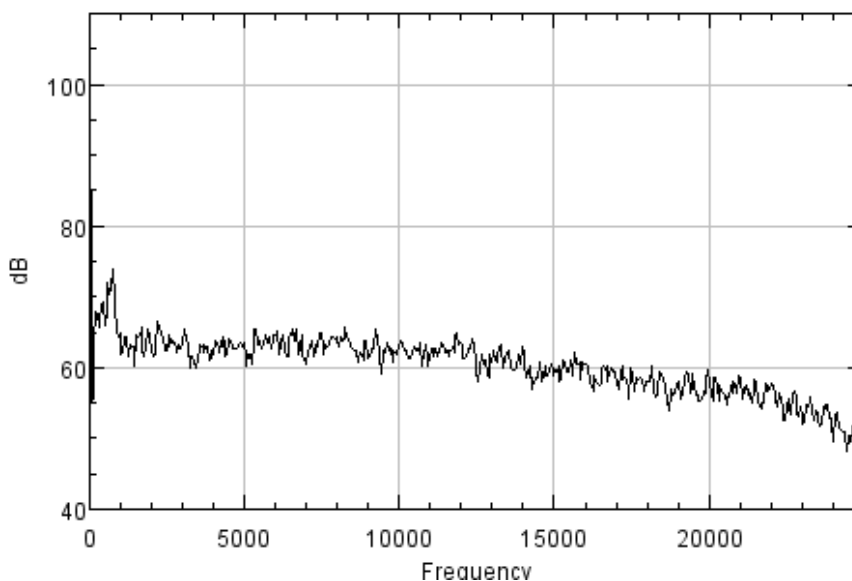


Figure 39: Square big vs spear spectrum, 0.5M

Once again, the only appreciable change in shape of the spectrum and in location and identification of sources is the general increase of noise level (again 5 dB approximately), although this time the peak at 9.8 kHz has disappeared and no noticeable peak is appreciated outside the normal louder noise at low frequencies. As it can be seen, the noise generation is quite uniform throughout all the frequency range:

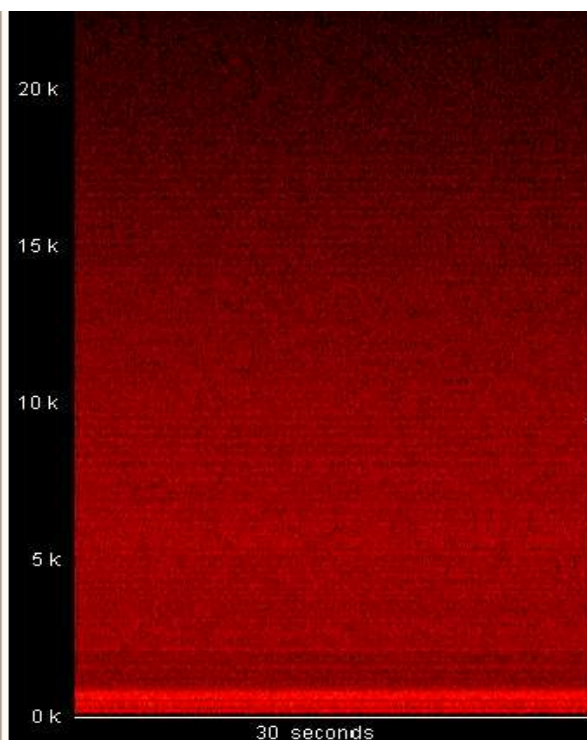


Figure 40: Square big vs spear spectrogram, 0.5M



4.5) 0.6M:

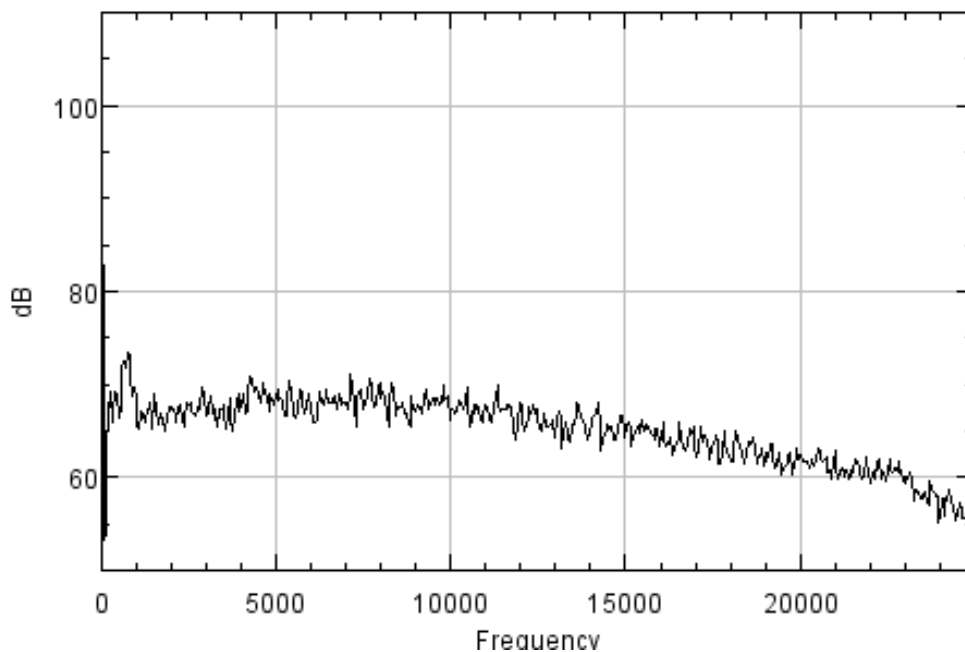


Figure 41: Square big vs spear spectrum, 0.6M

Nothing new in this last case, where once again all noise levels increase by about 5 dB but the shape and behavior is the same.

So, as a conclusion, it can be agreed that noise increase follows a linear behavior with respect to the flow speed, of about **5 dB noise increase per 0.1M speed increase**. With regards to the shape, it is clear that the spear has been identified as the source of noise peaks and louder noises.

5) Nozzle comparison: square small vs square big

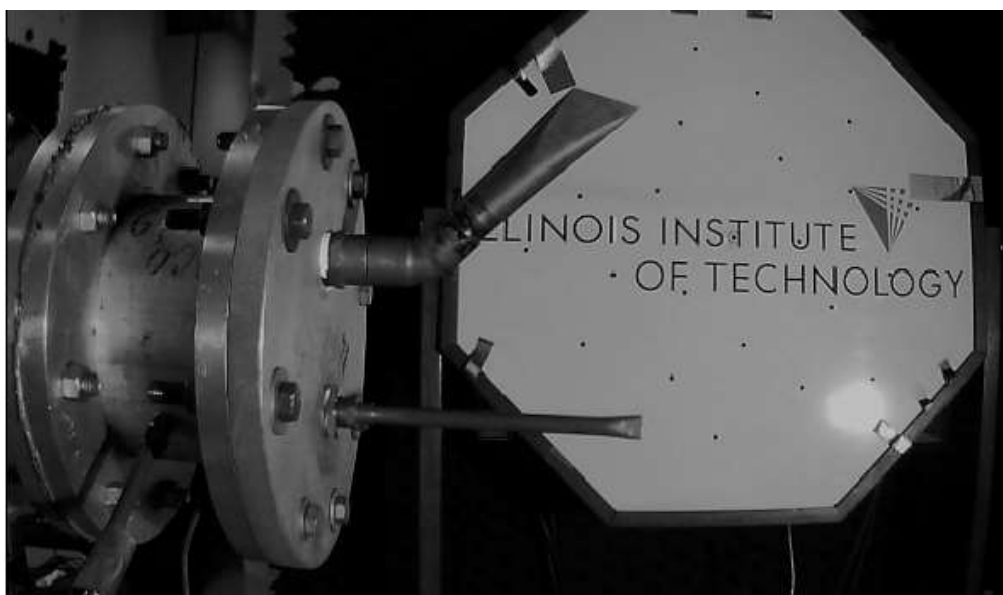


Figure 42: Squares comparison setup



5.1) 0.2M:

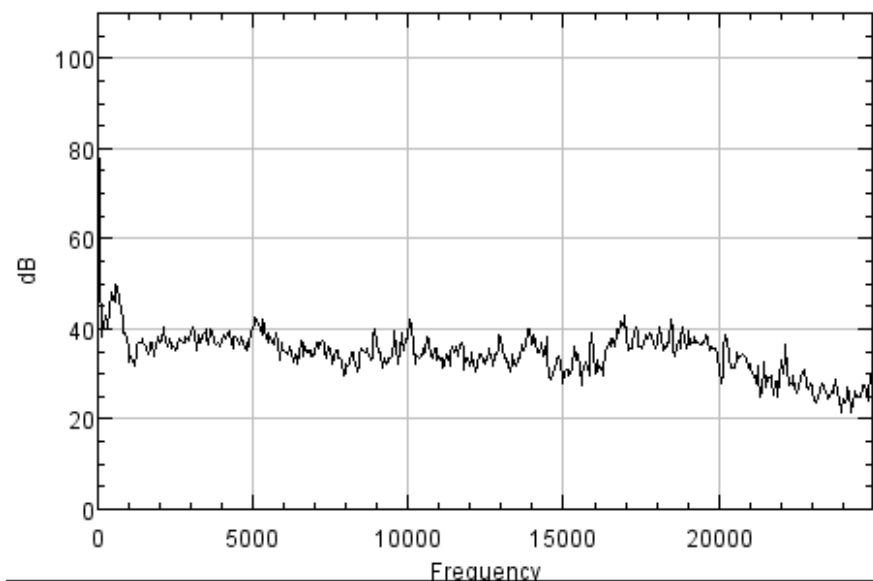


Figure 43: Squares spectrum, 0.2M

Taking a quick glance at the spectrum we can make ourselves an idea of the general shape and noise range that we can expect on this set of experiments. Being so, it appears clear again a normal spiky tendency but quite horizontal noise line, although it is as always louder in the lower frequency ranges than in the very high ones. However, we will see how the general noise level increases with flow speed. Throughout all ranges, it has been identified that the bigger square-shaped nozzle is the loudest noise source:

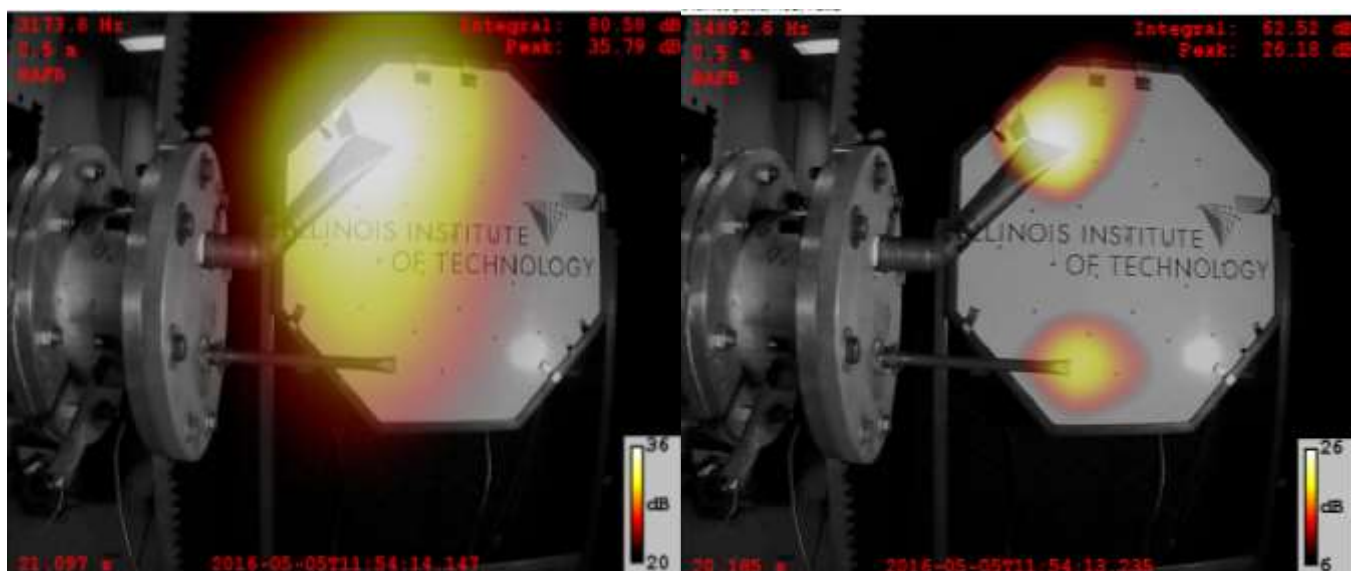


Figure 44: Square comparison, noise source identification



5.2) 0.3M:

The following spectrogram has been amplified in comparison to the previous one. However, although the “spikiness” is more evident now, a cold analysis proves that the behavior is just the same, with lower frequencies louder than high ones, but an increase in general “average” loudness somewhere between the 5 and 10 dB (although this increase is less uniform than with other nozzle geometries), and the noise source identification has given the same results as with 0.2M.

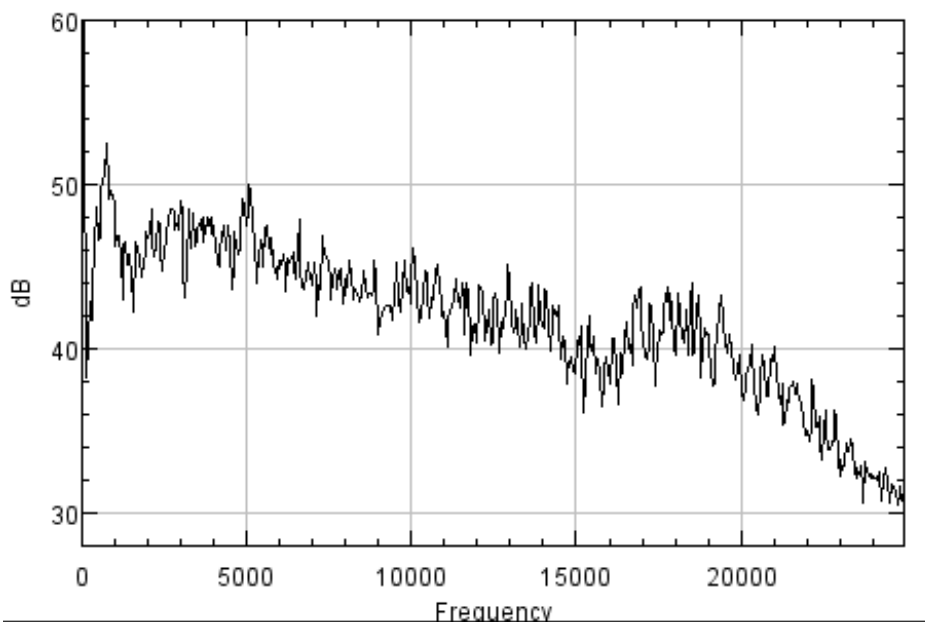


Figure 45: Squares comparison spectrum, 0.3M

5.3) 0.4M:

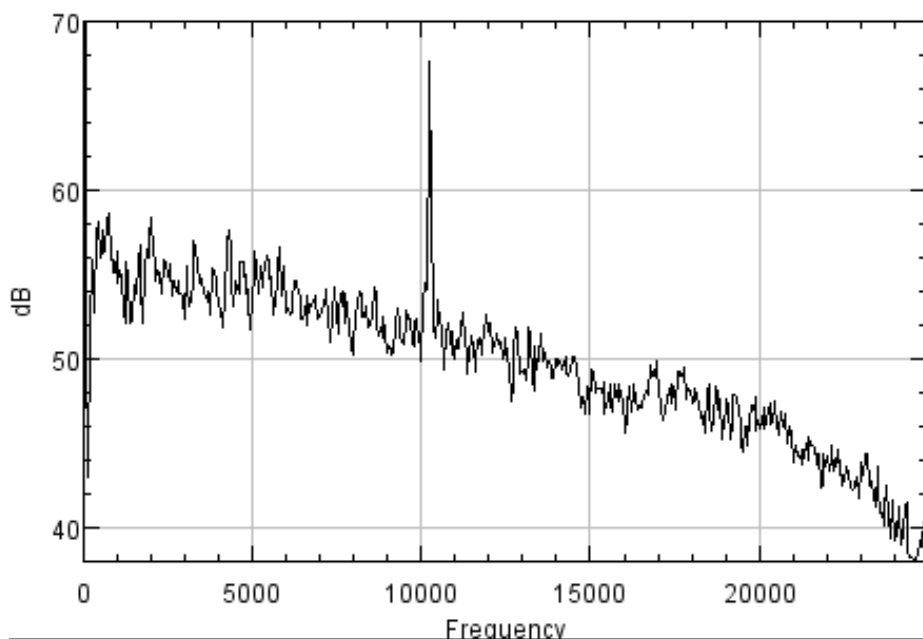


Figure 46: Squares comparison spectrum, 0.4M



There is a curious phenomenon happening at this flow speed: although the general behavior can be appreciated to be exactly the same as in previous experiments, this time there is a clear outstanding peak around 10.2 kHz, probably because at this flow speed some near-resonance vibration mode is triggered in the bigger square nozzle (identified as the source of this noise):

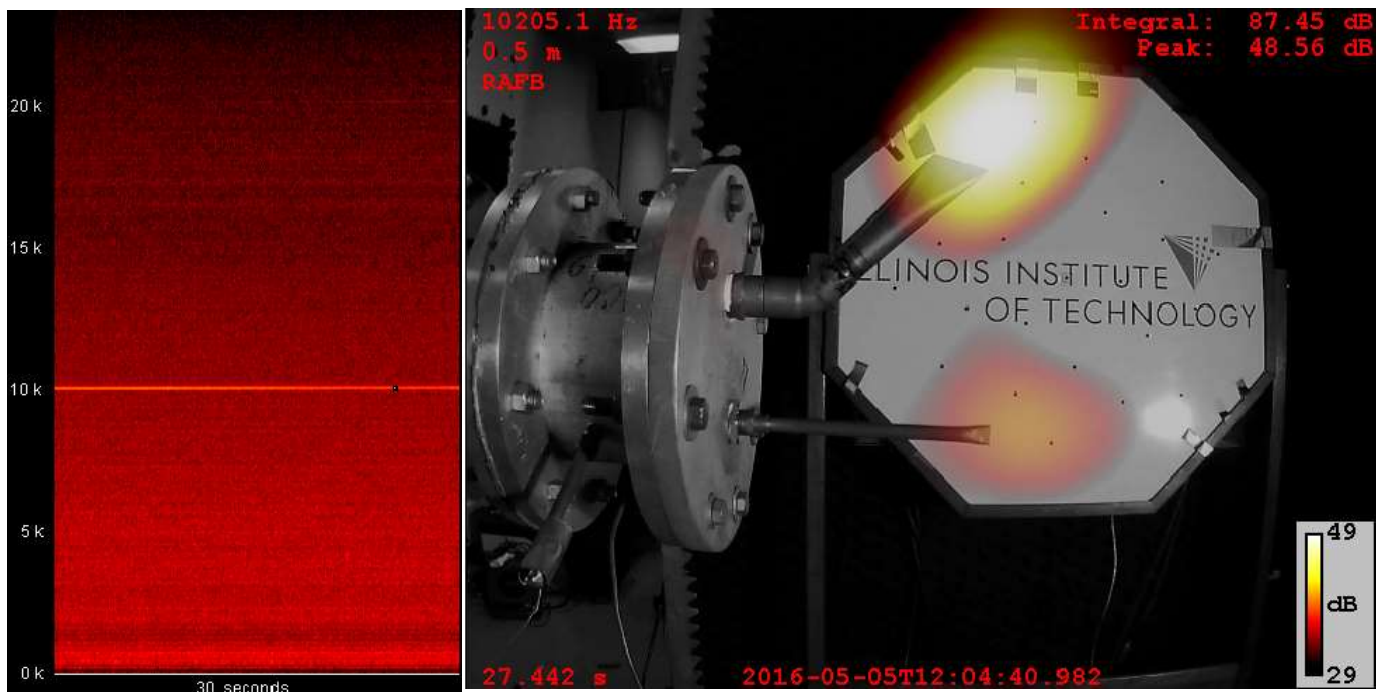


Figure 47: Squares comparison, 0.4M spectrogram and source identification

5.4) 0.5M:

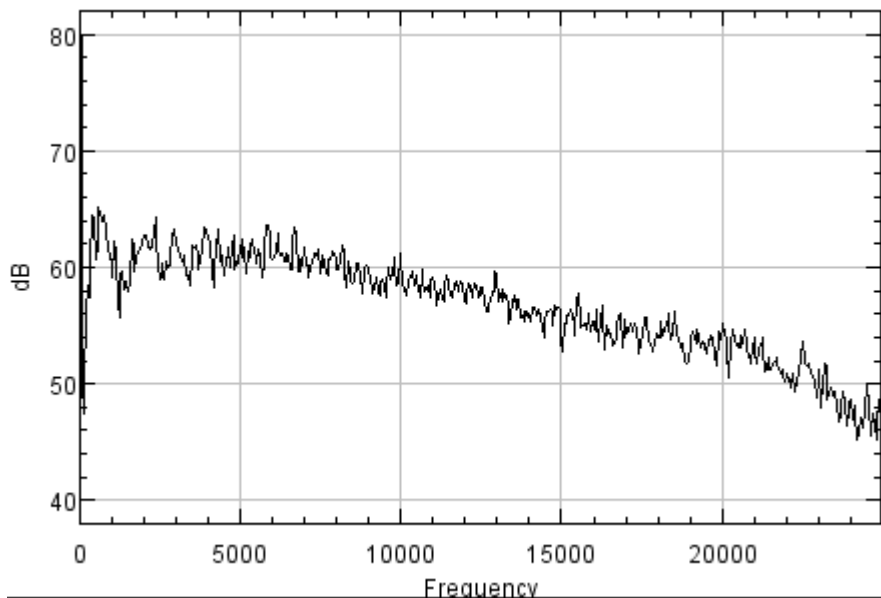


Figure 48: Squares comparison spectrum, 0.5M



Interestingly, the peak at 10.2 kHz has now disappeared, what supports the theory of a near-resonance vibration mode being triggered. There is not much else to comment apart from the usual seen effects and behavior.

5.5) 0.6M:

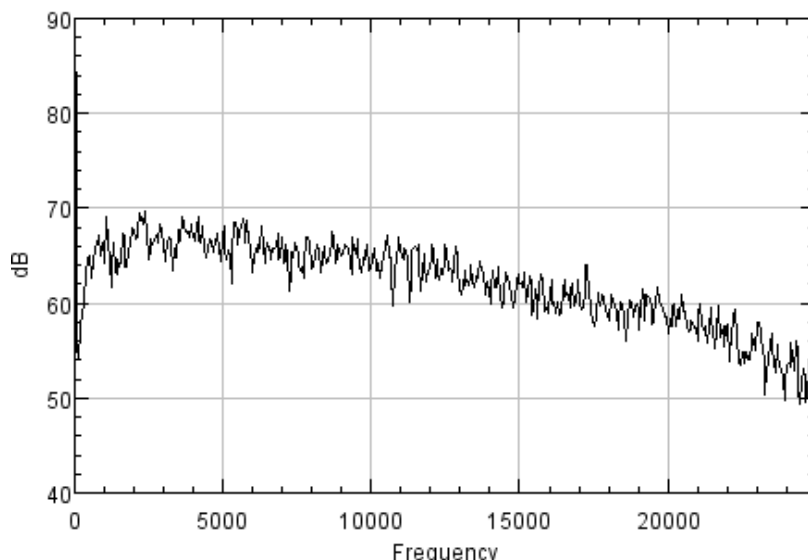


Figure 49: Squares comparison spectrum, 0.6M

Once again, in this last experiment can be seen the same tendencies and behavior that have been previously explained and so confirm our theories so far: that lower frequencies are always the loudest (in this case, starting around 65 dB in average and ending at 55 dB), but a somehow horizontally spiky line is followed. With regards of the nozzle comparison, the big square has always been identified as the noisiest source.

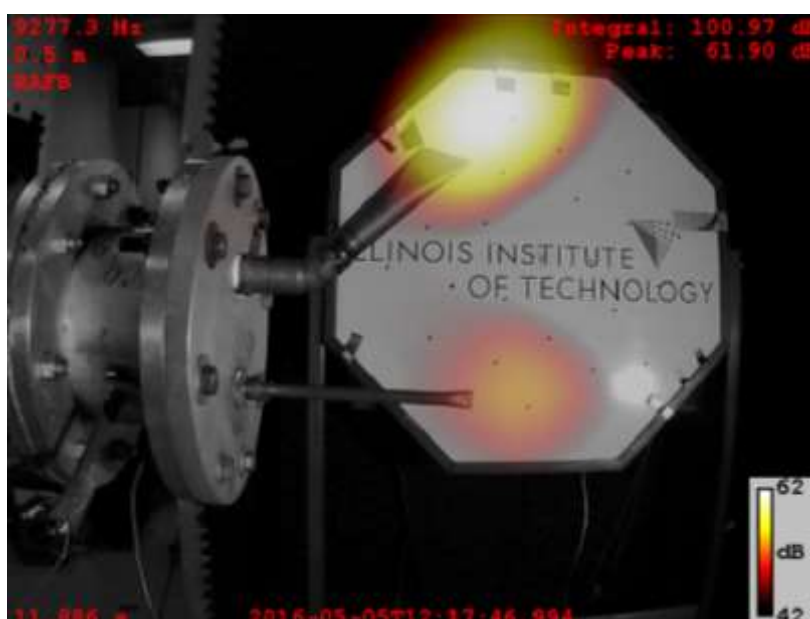


Figure 50: Squares source identification, 0.6M



6. Conclusions

Throughout all the experiments carried out and the background research, there are some important conclusions to be withdrawn. First of all, the current and increasing importance of aeroacoustics as a field inside engineering and science in general, with an important set of new applications that will only widen in the future as research and techniques keep on advancing.

Secondly, the high usefulness of the software BeamformX, the way to use it, and generally speaking the correct procedures and methodologies involving experiments in the field of aeroacoustics and the utmost importance of these in order to get good, accurate results not polluted by environmental noise etc. In this sense, the significance of good, appropriate facilities (as the insulation chamber).

With regards to the experiments results themselves, 3 main conclusions can be deduced. In first place, the general tendency line on the spectrums, by means that noise in low frequency ranges is somewhat higher than in high ranges, but this difference is never relatively great, and seen in a 20 – 90 dB range, to keep a human hearing reference, the tendency line remains spiky, but quite horizontal, “average wise” speaking, although sometimes outstanding noise peaks were found at certain flow speeds, probably because these triggered some near-natural frequencies of the nozzles.

Another important effect noted is the apparently linear relationship between flow speed and noise, being appreciated a sustained increase of roughly about 5 dB for every 0.1M flow speed increase at all experiments, although this behavior may probably be lost when near-supersonic speeds are reached and compressibility effects start arising. Such velocities were as explained not reached in these research for security reasons, but are subject of further research and study for the future.

Last, in all comparisons was seen how the nozzles with the greatest contact perimeter in the outlet were identified as the source of loudest noise, but the design of outlets and nozzles is determined by many considerations: mechanical, thermodynamic, ease to manufacture.... And noise generation is just one of the factors, but not the only nor most important one.